UKACC International Conference on Control 2012
Cardiff, UK, 3-5 September 2012

Research on a novel PID based controller for non-magnetic hydraulic navigation simulator with AMESim simulation

Zhou Kaibo, Wang Xuyong, Tao Jianfeng, Guo Xiaofeng, Xu Chuanhui
School of Mechanical Engineering
Shanghai Jiaotong University
Shanghai, China
zhoukaibo87@gmail.com

Abstract—**In this paper we research on the run time characteristics of non-magnetic hydraulic navigation simulator and approach a corresponding control strategy. Since the simulator is designed to be non-magnetic, it consists of long hydraulic pipes separating electric part and mechanical part to avoid the magnetic interference from electric part. Meanwhile the mechanical part is made of non-magnetic materials. Hydraulic motor, instead of electric motor, is used to drive the simulator and it stands varied load at run time. Because of the non-magnetic design, normal control strategy doesn't satisfy the system. We analyze the characteristics of the simulator system both in frequency-domain and time-domain with the help of transfer function and AMESim, which is a modeling environment for simulation of engineering, to make the characteristics clear and finally propose a PID based control strategy (denoted as D_{ff} - $PIDD^2$ in this paper) combining feedforward differential controller (D_{ff}) and 2nd order differential controller (D^2) for the system. At last we verify the control strategy with position tracking simulation and obtain a satisfied result.**

Keywords-non-magnetic; long-hydraulic pipe; navigation simulator; D_{ff} - $PIDD^2$; AMESim simulation

I. INTRODUCTION

Non-magnetic navigation simulator is a platform which is used to test and to calibrate magnetic navigation devices [1]. Magnetic navigation devices are widely used to obtain accurate direction data in various fields, such as military, aviation, aerospace, resource exploration, and etc. When being tested and calibrated, magnetic navigation device is installed in the middle of inner ring of the simulator (Fig. 1) and the direction data from magnetic navigation device will be compared with the precisely controlled rotation data of the simulator. The simulator we work on is designed for a magnetic navigation device which navigates depending on the geomagnetic field. The geomagnetic field is very small (6e-5T averagely) compared to common magnetic fields in our daily life and is easy to be deformed in space by some paramagnetic or diamagnetic media. Because of the special characteristics of the geomagnetic field, the simulator has to be designed without influencing the magnitude and direction of the geomagnetic field nearby.

To achieve the non-magnetic requirement, generally there are three driven schemes for navigation simulator: motor driven, pneumatic driven and hydraulic driven. Motor driven simulator requires separating the motor and the tested device to avoid the magnetic interference from electric motor. The non-magnetic motion simulator used by U.S. Coastal System Station is based on motor driven scheme [2]. Pneumatic driven avoids the magnetic interference in principle. The motion platform designed by University of Newcastle, UK, which is used to test high-precision magnetic device, is based on pneumatic driven scheme [3]. Hydraulic driven also in principle avoids the magnetic interference and the compressibility of hydraulic oil is much less than gas so that it is more likely to achieve high-precision positioning and fast motion tracking. Besides driven scheme, non-magnetic materials are necessity to construct the simulator. Some commonly used non-magnetic materials are austenitic stainless steel, copper alloy, polymers, ceramic material, and etc. [4].

The non-magnetic navigation simulator we designed is based on the hydraulic driven scheme and many other design features, which will be included in the next section, to achieve non-magnetic requirement. Because of the non-magnetic requirement, the run time characteristics of the system are quite different from normal navigation simulator and normal PID control strategy doesn't satisfy the system. In this paper we focus on the derivation of control strategy for the non-magnetic navigation simulator. And we focus more on the theoretical control scheme rather than real application details so that only the most important and crucial features of the system will be counted and some necessary supplementary control strategies for real application, e.g. using low-pass filter to eliminate high frequency noise signal from sensor, may be neglected in this paper. The performance of the derived control strategy will be verified by a simulated simulator system tracking a sine wave position singal with AMESim software.

National Natural Science Foundation of China [grant numbers 50975172, 50805090]
Research Fund of State Key Lab of MSV, China [grant number MSV-2010-05]

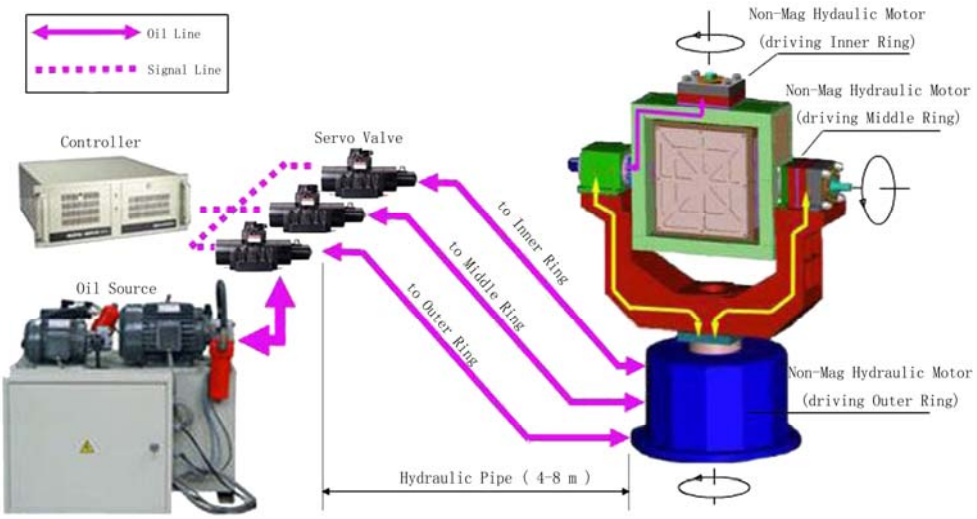

Figure 1. System composition of non-magnetic hydraulic navigation simulator

I. PRINCIPLE OF THE NAVIGATION SIMULATOR

The basic structure of the non-magnetic hydraulic navigation simulator system is shown in Fig. 1.

Generally we divide the system into the electronic control part and the mechanical part. They are connected by signal lines mainly including current signals from controller to servo valves and feedback angular displacement signals from angle sensors to controller. Angle sensor is mounted at the end of each non-magnetic hydraulic motor. The angle sensor on the simulator is a kind of optical encoder, which is a passive device and has an acceptable influence on geomagnetic field [5].

The fundamental principle of the whole system is close to a classic valve controlled hydraulic motor system. But there are several different features in this navigation simulator, which are mainly designed to achieve the non-magnetic requirement. These features are:

- We use beryllium bronze (Cu-Be-Co) [6] and other non-magnetic materials for hydraulic pipe and mechanical components of the navigation simulator;
- We use hydraulic motor made of non-magnetic materials instead of electric motor and optical angle sensor instead of electromagnetic sensor;
- In order to eliminate the electromagnetic interference from the servo valve and oil source side, we separate the mechanical part and the electric part by connecting them with long hydraulic pipes.

When the simulator runs, three servo valves independently control the rotation of three rings, which are known as pitch (outer ring), course (middle ring), and roller (inner ring). The controller outputs the current signals, which are computed based on the feedback angular displacement and our control strategy, to control the spool position of servo valve so that each ring can rotate at a set speed or to a set position.

II. MODELING WITH AMESIM

In order to know the run time characteristics of navigation simulator especially the influence of non-magnetic designs on the system and approach a suitable control strategy, we model and simulate the system with AMESim (Fig. 2). We set up two models for different reasons. The model with no controller is used to simulate the open-loop characteristic of the system and to check the characteristic of each component. The model with D_{ff} - PIDD^2 controller is to test the effectiveness of our control strategy and to simulate the open-loop characteristic of the controller-controlled system as well. During modeling we focus on the most important parts of the system to make the model neat and effective. Here are some instructions for the AMESim model of non-magnetic navigation simulator system:

- We set the oil source pressure to follow the equation of $p_s=95+5\sin(200\pi t)$ (bar) to simulate the pressure ripple caused by periodic rotation of pump at oil source side;
- To smooth the ripple and to keep a steady oil pressure inside the pipe we set up an accumulator right after oil source and the filter;
- We select a three-position-four-port servo valve, the spool dynamics of which is modeled as a 2nd order system with a specified natural frequency and damping ratio;
- The hydraulic pipe is modeled as distributive hydraulic line with lumped elements [7];
- Without losing the effectiveness of the model, we simply model the hydraulic motor as an ideal fixed displacement hydraulic motor and we only simulate one ring of the simulator because the three rings have similar characteristics and work independently;
- The rotary load is set with specified moment of inertia, coefficient of viscous friction, Coulomb friction torque, and stiction torque [8].

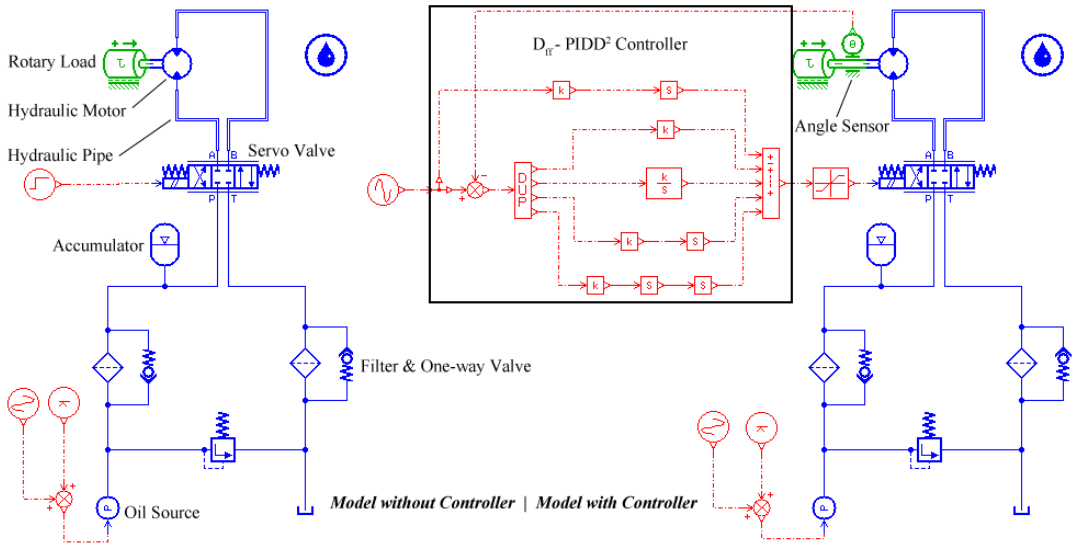

Figure 2. Model with no controller (left) and model with D_{ff} - PIDD^2 controller (right)

The distributive hydraulic line model describes the hydraulic pipe as line with several nodes (Fig. 3). The compressibility of the fluid and expansion of the pipe/hose wall with pressure are considered in the model by using an effective bulk modulus. Pipe friction is taken into account using a friction factor based on the Reynolds number and relative roughness. And inertia of the fluid is also taken into account. The parameters of the whole model are set in Table I.

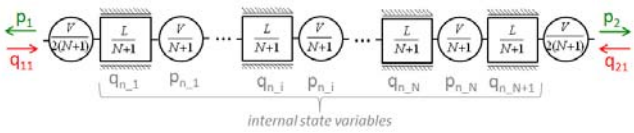

Figure 3. The principle of distributive hydraulic line model (Source: AMEHelp HL042)

TABLE I. PARAMETERS OF NON-MAGNETIC HYDRAULIC NAVIGATION SIMULATOR AMESIM MODEL

No.	Parameters	Value or Expression
1	Oil source pressure (bar)	95+5sin(200πt)
2	Accumulator volume (L)	6.3
3	Accumulator pre-charge pressure (bar)	80
4	Valve rated current (mA)	40
5	Valve nature frequency (Hz)	80
6	Valve damping ratio (null)	0.8
7	Valve flow rate at maximum opening (L/min)	10
8	Valve pressure drop at maximum opening (bar)	35
9	Pipe inner diameter (mm)	8
10	Pipe wall thickness (mm)	2
11	Pipe length (m)	5
12	Pipe relative roughness (null)	1.5e-4
13	Pipe Young's modulus (bar)	1.3e+6
14	Pipe internal node number (null)	5
15	Motor displacement (cm^3/rev)	80
16	Load moment of inertia (kgm^2)	5
17	Load viscous friction coefficient (Nm/[rev/min])	0.1
18	Load stiction torque (Nm)	4
19	Load coulomb friction torque (Nm)	2
20	Position tracking signal (degree)	40sin(πt)

III. SIMULATION AND ANALYSIS

A. *Fundamental analysis of the system*

As we mentioned in the principle section, the fundamental part of the system is a valve controlled hydraulic motor system. So firstly we study on the characteristics of this fundamental part in frequency-domain. The linearized flow rate incremental equation of hydraulic valve is defined as:

$$\Delta q_{Lv} = K_q \Delta x_v - K_c \Delta p_{Lv} \tag{1}$$

where q_{Lv} is flow rate, x_v is spool position, p_{Lv} is load pressure, K_q is flow rate gain, K_c is flow-pressure coefficient. Then we give out the expression of angular displacement of hydraulic motor directly [9]:

$$\theta_m(s) = \frac{\frac{K_q}{D_m}\frac{K_{sv}}{\frac{s^2}{\omega_{sv}^2}+\frac{2\zeta_{sv}}{\omega_{sv}}s+1} i_c(s) - \frac{K_{ce}}{D_m^2}(1+\frac{V_t}{4\beta_e K_{ce}}s)T_{ml}(s)}{s(\frac{s^2}{\omega_h^2}+\frac{2\zeta_h}{\omega_h}s+1)} \tag{2}$$

where i_c is current signal output by controller, T_{ml} is torque load reflected on hydraulic motor shaft, D_m is displacement of motor, K_{ce} is total flow-pressure coefficient, β_e is effective bulk modulus of motor system, ω_{sv} is servo valve natural frequency, ζ_{sv} is servo valve damping ratio, K_{sv} is servo valve gain, ω_h is hydraulic natural frequency, ζ_h is hydraulic damping ratio.

In order to reduce the complexity of the model, we temporarily make the assumption $T_{ml}(s) = 0$, which means motor load is zero for the moment. Then (2) reduces to

$$\frac{\theta_m(s)}{i_c(s)} = \frac{K_q K_{sv}/D_m}{s(\frac{s^2}{\omega_h^2}+\frac{2\zeta_h}{\omega_h}s+1)(\frac{s^2}{\omega_{sv}^2}+\frac{2\zeta_{sv}}{\omega_{sv}}s+1)} \tag{3}$$

It can be seen from (3), if we neglect the long hydraulic pipe and assume zero motor load, the model with no controller is a first order astatic system with two oscillation elements, which can be theoretically regulated by a PID controller [10].

B. *Analysis of hydraulic motor load*

The second step we take the hydraulic motor load into account. The motor load is defined as:

$$T_{ml} = C_1\dot{\omega}_m + C_2\omega_m + C_3(1-|\operatorname{sgn}(\omega_m)|) + C_4 \tag{4}$$

where ω_m is the angular velocity of motor, C_1, C_2, C_3, and C_4 are constants defined in Table I (No. 16-19). The transfer function of the system will become very complicated when combining (2) and (4), and it will be difficult to draw a proper control strategy. So we analyze the system in time-domain based on AMESim simulation result.

The motor load influences the system by changing the load pressure, i.e. the pressure difference between the inlet and outlet of motor. Recalling (1), we see if the opening amount of valve spool keeps unchanged while the load pressure increases/decreases, the flow through the motor will reversely decrease/increase. In order to eliminate the varied motor load influence on the flow rate, we introduce compensation current to simultaneously act on the opening amount of spool. According to (4) we need to involve angular velocity and acceleration of the motor and a constant into control signals. Because the velocity signal is already able to be reflected in the PID controller and the constant is relatively small compared to other terms in (4), we only introduce an extra 2nd order differential controller (D^2) to get the acceleration of the motor. Through the simulation of model with D_{ff} - PIDD^2 controller tracking a sine wave position signal in AMESim (detailed simulation parameters will be included in later section), it can be seen from Fig. 4 that the simulated output of D^2 controller is always in the same pace with the motor load and reflects the acceleration of motor.

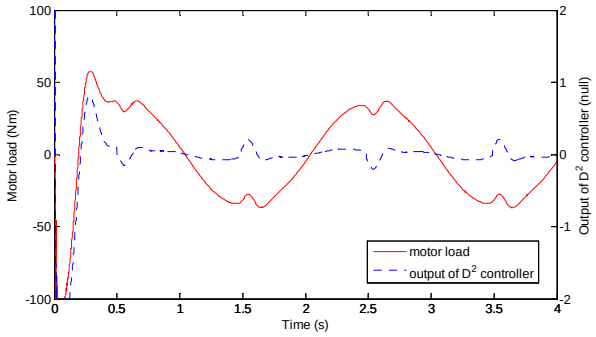

Figure 4. Comparison of motor load and D^2 controller output in model with D_{ff} - PIDD^2 controller

C. *Analysis of long hydraulic pipe*

At last we research on control strategy with long hydraulic pipe taken into consideration. The distributive hydraulic line model describes the pipe as a line with several nodes and calculates the pressure and flow rate in each node with the following equations (Source: AMEHelp HL042):

$$\begin{cases} \dfrac{\partial p_p}{\partial t} = -\dfrac{\beta_{ep}}{A_p}\cdot\dfrac{\partial q_p}{\partial x} \\ \dfrac{\partial q_p}{\partial t} = \dfrac{A_p}{\rho}\cdot\dfrac{\partial p_p}{\partial x} - gA_p\sin(\theta_p) - v\dfrac{\partial q_p}{\partial x} - \dfrac{f_f q_p^2 \operatorname{sgn}(q_p)}{2D_p A_p} \end{cases} \tag{5}$$

where p_p is pressure in node, q_p is flow rate in node, A_p is the cross-sectional area of pipe, β_{ep} is the effective bulk modulus of pipe/fluid combination, ρ is the oil density, D_p is the diameter of the section of pipe, θ_p is the inclination of pipe, v is the mean velocity of flow in node, f_f is the friction factor of node.

It can be seen that, the derivative of the flow rate is determined by applying conservation of momentum principles to a control volume cell. Forces due to pressure, gravity and pipe friction are taken into account as well as convection of momentum. And we again analyze the pipe effect in time-

domain. As shown in Fig. 5, through the simulation of model with no controller tracking a step position signal, the simulated flow rate in hydraulic motor delays about 0.2 second compared to flow rate at port A of the servo valve.

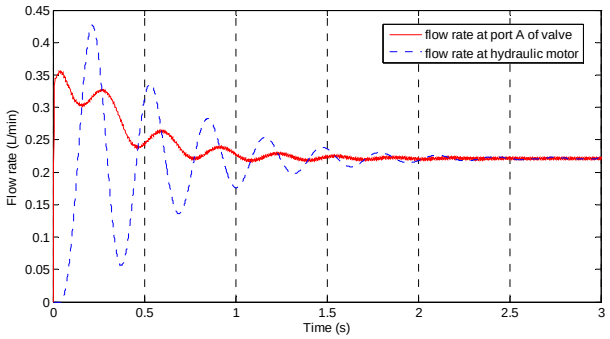

Figure 5. Flow rate in model with no controller

Because pipe is the only component connecting motor and servo valve, it is obviously that the long hydraulic pipe causes the time delay. It means if we could give out the tracking signal a certain time period in advance, we are able to cancel the flow rate delay in pipe. We now assume the tracking signal can be described as a continuous differentiable function f(t), then for $t_B > t_A$ and $t_B - t_A << 1$ we have

$$\begin{aligned} f(t_B) &= f(t_A + t_B - t_A) \\ &= f(t_A) + f'(t_A)(t_B - t_A) + f''(t_A)(t_B - t_A)^2 + \cdots \end{aligned} \tag{6}$$

Since $t_B - t_A << 1$, we neglect the terms with order equal to or higher than 2. Equation (6) reduces to

$$f(t_B) - f(t_A) \approx f'(t_A)(t_B - t_A) \tag{7}$$

Equation (7) shows that we can approach the incremental of signal at t_B to signal at t_A with the derivative of signal at t_A. Inspired by this equation we introduce the feedforward differential controller (D_{ff}) into control strategy:

$$D_{ff} = Ks \tag{8}$$

Compared to (7), we roughly have gain $K = t_B - t_A$.

D. Overall control strategy and simulation result

Combining all above analysis, we draw the overall control strategy for the system. We use a PID controller as fundamental control strategy together with a D^2 controller regulating the hydraulic motor load fluctuation and a D_{ff} controller eliminating time delay effect caused by long hydraulic pipe. In order to check the effectiveness of the controllers, we simulate a position tracking test in AMESim. The tracking signal is set to be a sine wave position signal described in Table I (No. 20), which meets the non-magnetic simulator specification. The result of the simulation test is shown in Fig. 7 with controller parameters in Table II.

Through the comparison between D_{ff} - PID control and PID control, we see the D_{ff} controller effectively eliminates the time delay of the system. Through the comparison of PIDD^2 control and PID control, we see the D^2 controller reduces the tracking error fluctuation of the system at start stage, during which the motor load changes rapidly and greatly (Fig. 4). Because our system stands varied motor load and the feedback signal is angular displacement of motor, the D^2 controller precisely catches the load fluctuation and compensates it to the control current signal. D^2 controller is rarely seen in traditional control strategy because it usually introduces instability to system. In real applications a low-pass filter might be used to eliminate high frequency noise signal from sensor.

Besides the time-domain analysis with AMESim, we also do a frequency-domain test (Bode diagram) of the two models in open-loop state. We analyze the stability of the two models based on Bode diagram stability criterion for open-loop system (Fig. 6) [11]. This criterion defines the magnitude crossover frequency (ω_{mc}) as the frequency where the magnitude is equal to 0 and the phase crossover frequency (ω_{pc}) as the frequency where phase shift is equal to -180 degree. If at the phase crossover frequency, the corresponding magnitude is less than 0 dB, then the feedback system is stable. According to Bode diagram criterion (using the vertical lines in Fig. 8 as reference), the model with no controller is not stable while the model with controller is stabilized. The diagram also shows that model with D_{ff} - PIDD^2 controller has faster response in low frequency region and broader frequency band without phase delay. Although the attenuation of model with controller in high frequency region becomes slower, it is within an acceptable amount.

TABLE II. CONTROLLER PARAMETERS FOR SINE POSITION TRACKING SIMULATION

Controller	PID	PIDD^2	D_{ff} - PID	D_{ff} - PID
D_{ff}	null	null	0.05	0.05
P	0.6	0.6	0.6	0.6
I	0.5	0.5	0.5	0.5
D	0.05	0.05	0.05	0.05
D^2	null	0.002	null	0.002

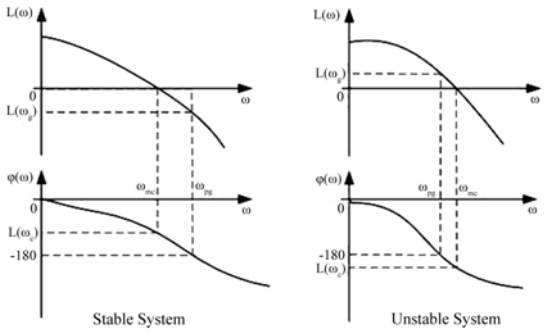

Figure 6. Bode diagram stability criterion for open-loop system

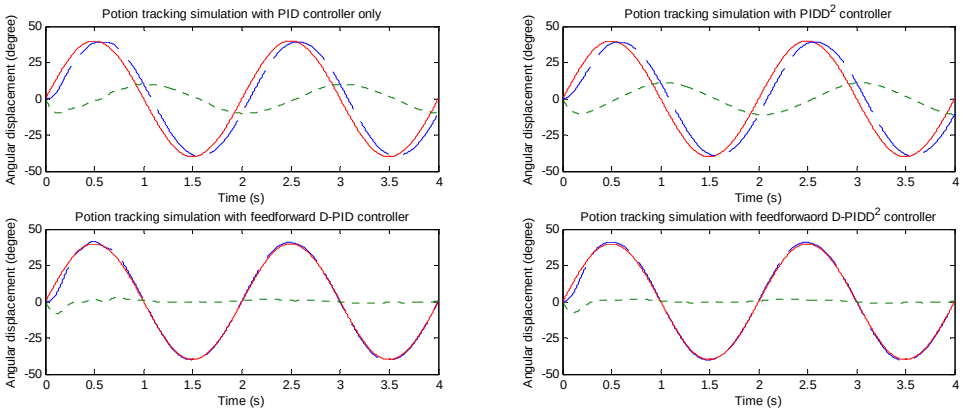

Figure 7. Simulation result of sine position signal tracking (solid line: target signal, dashed line: tracking result, dense dashed line: tracking error)

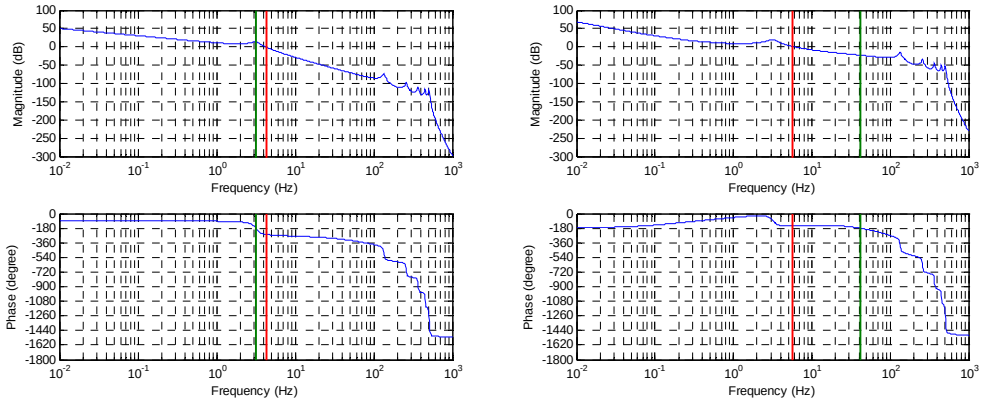

Figure 8. Bode diagram of model with no controller (left) and model with D_{ff}-PIDD^2 controller (right)

IV. CONCLUSION

Through modeling, simulation and analysis of non-magnetic hydraulic navigation simulator, we conclude that the simulator is a time-delay valve controlled hydraulic motor system with varied motor load. We firstly focus on the most fundamental parts of the system, i.e. valve controlled hydraulic motor, which is a common hydraulic system and on which mature control strategy can be applied. Secondly we analyze the special parts of the system in time-domain with simulation results. During this process we isolate each component and come up with different control strategies. Finally we propose the D_{ff} - PIDD^2 controller for the system, which is proven more effective than the traditional PID controller theoretically and with simulation as well. The D_{ff} - PIDD^2 controller may also be applied to real applications of similar system with time delay or varied force/torque load.

REFERENCES

[1] L. A. DeMore, R. A. Peterson, L. B. Conley, and et al., "Design study for a high-accuracy three-axis test table," Journal of Guidance, 1987, 10(1): 104-114.

[2] George I. Allen, John Purpura, David Overway, "Measurement of magnetic noise characteristics on select AUVS with some potential mitigation techniques," OCEANS '02 MTS/IEEE. 2002, 9782-9978.

[3] Kevin P. Humphrey, Thomas J. Horton, Mark N. Keene, "Detection of mobile targets from a moving platform using an actively shielded, adaptively balanced SQUID gradiometer," IEEE Transaction on applied superconductivity. 2005, 15(2): 753-756.

[4] K.H.J. Buschow. Handbook of Magnetic Materials, vol 18. North Holland Press, 2009.

[5] Kenneth Schofield, Desmond J. O'Farrell, Kenneth L. Schierbeek, Magnetic compass with optical encoder. US4937945, Jul 3 1990.

[6] Ana Galet, Ana Belén Gaspar, M. Carmen Muñoz, and et al., "Tunable bistability in a three-dimensional spin-crossover sensory- and memory-functional material," Advanced Materials, Volume 17, Issue 24, pages 2949–2953, December, 2005.

[7] Kong Xiaowu, Qiu Minxiu, "A study of the influences of pipe on valve control hydraulic system," Proceedings of the 5th International Conference on Fluid Power Transmission and Control. Hangzhou: Zhejiang University Press, 2001:23-27.

[8] Valentin L. Popov, Contact Mechanics and Friction: Physical Principles and Applications. Springer, 2010.

[9] Yang Zhengrui, Hua Keqin, Xu Yi, Electro-hydraulic Propotional and Servo Control. Beijing: Metallurgical Industry Press, 2009.8.

[10] Wang Xianzheng, Chen Zhenghang, Wang Xuyong, Control Theory. Beijing: Science Press, 2000.

[11] Benjamin C. Kuo, Farid Golnaraghi, Automatic Control Systems. John Wilev & Sons, 2003.